

## Contouring aspheric surfaces using two-wavelength phase-shifting interferometry †

KATHERINE CREATH, YEOU-YEN CHENG  
and JAMES C. WYANT

University of Arizona, Optical Sciences Center, Tucson,  
Arizona 85721, U.S.A.

*(Received 28 May 1985)*

**Abstract.** Two-wavelength holography and phase-shifting interferometry are combined to measure the phase contours of deep wavefronts and surfaces, such as those produced by aspherics, with a variable sensitivity. When interference fringes are very closely spaced, the phase data contain high frequencies where  $2\pi$  ambiguities cannot be resolved. In this technique, the surface is tested at a synthesized longer equivalent wavelength. The phase of the wavefront is calculated modulo  $2\pi$  using phase-shifting techniques at each of two visible wavelengths. The difference between these two phase sets is the phase of the wavefront as it would be measured at  $\lambda_{\text{eq}} = \lambda_1 \lambda_2 / |\lambda_1 - \lambda_2|$ , assuming that  $2\pi$  ambiguities can be removed at  $\lambda_{\text{eq}}$ . This technique enables surfaces to be contoured to an accuracy of  $\lambda_{\text{eq}}/100$ .

### 1. Introduction

Two-wavelength holography (TWH) and phase-shifting interferometry (PSI) are techniques for nondestructively testing optical components [1-3]. TWH uses two visible wavelengths to produce a long effective wavelength for wavefront contouring. It is a good technique for testing aspheres and steep surfaces because of its variable sensitivity; however, it is not very precise, and requires an intermediate holographic recording. PSI measures the phase of a wavefront using a single wavelength with very high measurement precision. Surface height variations can be determined from the phase data by using computers to record data and calculate surface errors. This technique is fast, has no intermediate recording step, or the inconvenience of using photographic chemicals.

Two-wavelength phase-shifting interferometry (TWPSI) is a technique which extends the measurement range of single-wavelength phase-shifting interferometry: it allows the measurement of profiles of deeper surfaces than has previously been possible with a single wavelength, by applying phase measurement to two-wavelength holography. TWPSI calculates the phase of the final 'hologram' from primary interferogram data inside the computer. A recent paper introduced this technique [4], and showed examples of one-dimensional measurements. This paper presents a different method, which is both simple and easy to calculate, for obtaining the same information in two dimensions.

† This paper is dedicated to W. H. Steel, whose writings demonstrate a significant contribution to optics.

‡ Present address: Jet Propulsion Laboratory, Pasadena, California, U.S.A.

## 2. Theory

In two-wavelength holography the interferogram at one wavelength  $\lambda_a$ , is recorded on photographic film with the test surface in place. It is then developed, placed back in the original position, and illuminated with the interferogram of the same surface but produced by a different wavelength  $\lambda_b$ . The interference pattern between these two interferograms is then spatially filtered to remove unwanted components. The result is an interferogram in which the fringes are spaced as if the surface were tested with an equivalent wavelength given by [1]

$$\lambda_{\text{eq}} = \frac{\lambda_a \lambda_b}{|\lambda_a - \lambda_b|}. \quad (1)$$

The sensitivity of the test can be varied by changing the two illuminating wavelengths. When the wavelengths used are produced by argon-ion and He-Ne lasers, the equivalent wavelength can be varied over the range 2 to 50  $\mu\text{m}$ .

Phase-shifting interferometry is a technique which can determine the shape of a surface or wavefront by calculating a phase map from the measured intensities. The phase information is obtained by shifting the phase of one beam of the interferometer by a known amount and measuring the intensity in the interferogram for many different phase shifts. For the single-wavelength PSI used in this study, the intensity was integrated over the time taken to move a reference mirror linearly using a piezoelectric transducer (PZT) through a 90° change in phase. Three frames of intensity data are recorded in this manner [2,3]:

$$\left. \begin{aligned} A(x, y) &= I_0[1 + \gamma[\cos(\phi(x, y)) - \sin(\phi(x, y))]], \\ B(x, y) &= I_0[1 + \gamma[-\cos(\phi(x, y)) - \sin(\phi(x, y))]], \\ C(x, y) &= I_0[1 + \gamma[-\cos(x, y) + \sin(\phi(x, y))]], \end{aligned} \right\} \quad (2)$$

where  $I_0$  is the average intensity and  $\gamma$  the modulation of the interference term. The phase  $\phi$  is calculated by [2,3]

$$\phi(x, y) = \arctan \left[ \frac{C(x, y) - B(x, y)}{A(x, y) - B(x, y)} \right]. \quad (3)$$

This equation is applied at each detector point recorded in the interferogram. The signs of the numerator and denominator determine which quadrant the phases are placed in. The optical path difference (OPD) between the reference and object wavefronts can be found from the phase by

$$\text{OPD}(x, y) = \frac{\phi(x, y)\lambda}{2\pi}. \quad (4)$$

This OPD is related to the object surface height by a multiplicative factor, which is 1/2 for a double-pass interferometer such as the Twyman-Green. Two-pi ambiguities are smoothed by comparing adjacent pixels and adding or subtracting  $2\pi$  until the difference between adjacent pixels is less than  $\pi$ . The phase of the wavefront between adjacent pixels must not change by more than  $\pi$  (one half-wave of OPD) for the  $2\pi$  ambiguities to be handled correctly. This restriction will limit the number of fringes which can be measured across the test surface, and thus limit the sensitivity of this test.

The two techniques can be combined to extend the sensitivity of phase-shifting interferometry to the range of two-wavelength holography [4]. This extension can be achieved by looking more closely at TWH.

Wyant shows that the interferogram obtained with two wavelengths has an intensity distribution given by [1]

$$I(x, y) = 1 + \cos \left[ 2\pi \text{OPD}(x, y) \left( \frac{1}{\lambda_a} - \frac{1}{\lambda_b} \right) \right]. \quad (5)$$

The expression assumes unit amplitudes and no tilt between the object and reference beams. The phase is given by the argument of the cosine term and can be written as

$$\phi_{\text{eq}}(x, y) = \frac{2\pi \text{OPD}(x, y)}{\lambda_{\text{eq}}} = \phi_a(x, y) - \phi_b(x, y), \quad (6)$$

where  $\phi_a$  and  $\phi_b$  are the phases measured for  $\lambda_a$  and  $\lambda_b$ . Thus, the difference of the phases measured at the two wavelengths will yield the phase associated with the equivalent wavelength. This approach is very simple, and easily implemented using existing phase-measurement equipment. In order to remove  $2\pi$  ambiguities from the equivalent wavelength data, the phase difference between two adjacent pixels of the equivalent phase must be less than  $\pi$ .

In a recent paper [4], Cheng used the following expression to calculate the wavefront OPDs from the calculated phases at each wavelength:

$$\Delta \text{OPD}_{n+1} = \frac{1}{2\pi} [\Delta \phi_{(n+1)b} - \Delta \phi_{(n+1)a}] \lambda_{\text{eq}}; \quad \lambda_a > \lambda_b. \quad (7)$$

where  $n$  refers to a pixel number in the detector array, and  $\Delta \phi_{n+1} = \phi_{n+1} - \phi_n$ . The OPD at the  $n$ th pixel is found by summing all of the  $\Delta$  OPDs up to the current pixel,

$$\text{OPD}_n = \sum_{m=1}^n \Delta \text{OPD}_m, \quad (8)$$

where the phase and OPD of the first pixel are set to zero. When this sum is evaluated, the resultant OPD at the  $n$ th pixel may be written as

$$\text{OPD}_n = \frac{\phi_{nb} - \phi_{na}}{2\pi} \lambda_{\text{eq}},$$

or

$$\phi_{\text{eq}} = \phi_{nb} - \phi_{na} = \frac{2\pi \text{OPD}_n}{\lambda_{\text{eq}}}. \quad (9)$$

This expression is the same as that given in equation (6) for  $\phi_{\text{eq}}$ . Thus, the same quantity is being calculated in both cases. However, the method outlined in this paper requires fewer calculations. Owing to the summation, equation (9) is sensitive to round-off errors. These errors can be avoided if phases are summed rather than OPDs.

There is another problem besides  $2\pi$  ambiguities which must be overcome in order to make two-wavelength measurements work. The PZT linear ramping voltage must have a different slope for each wavelength to ensure that the phase is shifted by  $90^\circ$  in each case. Equations that are independent of the amount the phase is shifted can be used to calculate the phase. Carré [5] presented a means of calculating

phase which assumes that the arbitrary phase shift  $2\alpha$  is constant between data frames and that the shift is linear. For this calculation, four intensities are recorded at each detector element:

$$\left. \begin{aligned} A(x, y) &= I_0[1 + \gamma \cos(\phi(x, y) - 3\alpha)], \\ B(x, y) &= I_0[1 + \gamma \cos(\phi(x, y) - \alpha)], \\ C(x, y) &= I_0[1 + \gamma \cos(\phi(x, y) + \alpha)], \\ D(x, y) &= I_0[1 + \gamma \cos(\phi(x, y) + 3\alpha)]. \end{aligned} \right\} \quad (10)$$

The phase calculated from these intensities is

$$\phi = \arctan \left[ \frac{\sqrt{\{(A-D) + (B-C)\}[3(B-C) - (A-D)]\}}}{(B+C) - (A+D)} \right]. \quad (11)$$

This method of calculating the phase involves more calculations than equation (3), and will therefore take more computing time; however, it will be more accurate and can be used for any wavelength without changing the PZT calibration.

A computer algorithm was written to calculate the phase using Carre's equations for each wavelength. After these phases were calculated, their difference was found and account taken of  $2\pi$  ambiguities. During the phase calculations, saturated data points and points where the modulation of the intensity is small were neglected.

The fundamental limit to this technique is the ratio of the detector size to the fringe spacing. If many fringes are incident upon a single detector element, the intensity measured will be an average over the detector area. When the phase is shifted, these points will not be modulated sufficiently that an accurate phase reading can be obtained. In the examples shown in the next section, there are detector points where this occurs. These points are discarded during the calculations. To avoid this problem, the size of the detector should be small compared to the fringe spacing. This ensures the sampling of one fringe at a time as the phase is shifted. The spacing between detectors determines the ultimate measurement sensitivity because of the  $2\pi$  ambiguities; but this can be overcome by simply changing the equivalent wavelength.

The largest errors in the phase maps can be attributed to chromatic aberration. Any glass elements in the interferometer should be achromatized for the wavelengths in use. A small amount of chromatic aberration can be tolerated, but it should not move the fringes or change the size of the interferogram by more than a pixel in order that good results can be obtained.

The sensitivity of TWPSI is limited by the equivalent wavelength used. Since PSI is generally accurate to  $\lambda/100$ – $\lambda/1000$ , this test should measure defects of the order 100–1000 Å for  $\lambda_{eq} = 10 \mu\text{m}$ . Because the data from two wavelengths are combined, there is an error magnification in effect. This means that the two-wavelength test will not give results as precise as a single-wavelength test, even though both have the same accuracy. In order to increase the sensitivity and precision at the same time, the single-wavelength  $2\pi$  ambiguities should be removed by taking the integrated two-wavelength phase [4].

### 3. Experiment

To illustrate this two-wavelength technique, the phases of many steep wavefronts were measured. A Twyman-Green interferometer (figure 1) with argon-ion

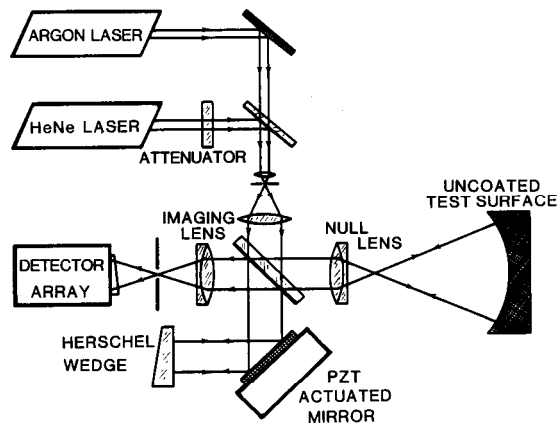
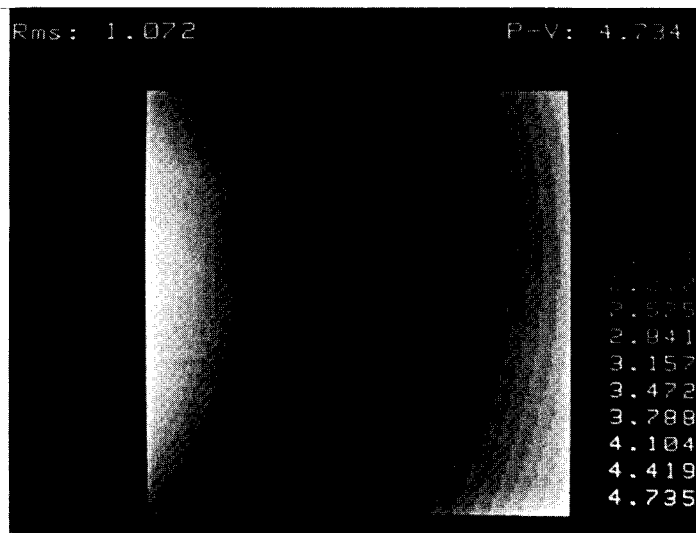


Figure 1. Experimental set-up for testing an uncoated aspheric surface using two-wavelength phase-shifting interferometry.

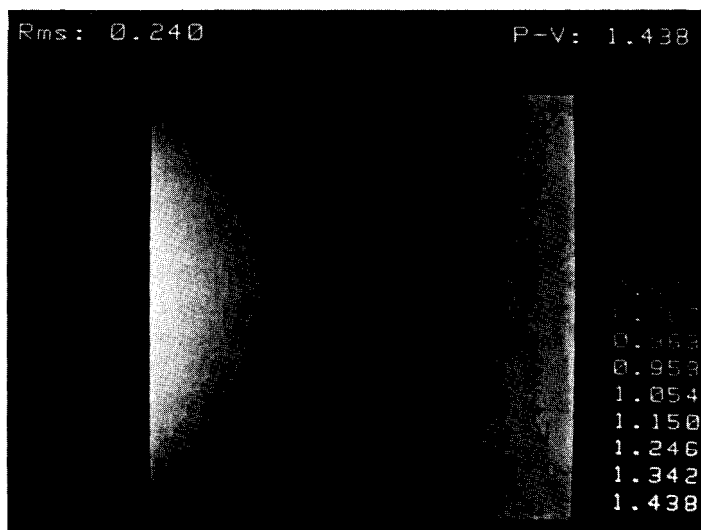
and He-Ne laser sources was aligned so that the beams of the two sources were colinear before the collimating optics. An uncoated test surface was placed in one arm of the interferometer, and a flat mirror controlled by a PZT placed in the other. A null lens was used to match the curvature of the base sphere for the aspheric surface. Interferograms were recorded using a Reticon  $100 \times 100$  diode array coupled to an HP-9836C computer. The number of fringes on the detector was controlled by positioning the detector and imaging lens. The wavelengths used in this experiment were either  $0.4880 \mu\text{m}$  or  $0.5145 \mu\text{m}$  from the argon-ion laser, combined with  $0.6328 \mu\text{m}$  from the He-Ne laser, to yield equivalent wavelengths of  $2.13 \mu\text{m}$  and  $2.75 \mu\text{m}$ .

Figure 2 shows the phase maps obtained by testing an aspherical surface with the tilt subtracted. The results of using single-wavelength PSI at  $0.6328 \mu\text{m}$  are shown in figure 2 (a), where the gray levels indicate the surface heights. The interferogram has roughly 4.7 waves of surface departure (9.5 waves of wavefront OPD) across the aperture of the detector for  $0.6328 \mu\text{m}$ . Figure 2 (b) shows the phase map obtained using the TWPSI technique on the same object and detector position. The number of waves peak-to-valley (P-V) for this phase map is 1.44 at  $2.13 \mu\text{m}$ . This number does not scale with the number of waves present in the one-wavelength measurement, and the two-wavelength result is noisier. Both these effects are due to chromatic aberrations in the lenses and the beamsplitter which can be seen to change the tilt and focus of the two single-wavelength interferograms. This problem can be reduced by removing the null and imaging lenses. The two-wavelength result of measuring the defocus due to a spherical surface shows much smoother contour levels and no visible tilt or defocus (see figure 3). The 1.90 waves P-V at  $2.75 \mu\text{m}$  scale correctly to give the 8.23 waves P-V at  $0.6328 \mu\text{m}$ . However, the null and imaging lenses have to be present to provide meaningful test results.

The power of this technique becomes evident when steeper wavefronts from the aspheric surface are contoured. With the lenses replaced and the detector positioned so that the fringe pattern is too fine for the detector array to resolve, a moire pattern is seen on the array. This is due to undersampling of the interference pattern by the detector array. The single-wavelength phase map (figure 4(a)) shows that the  $2\pi$  ambiguities could not be removed correctly owing to greater than  $\pi$  phase differences

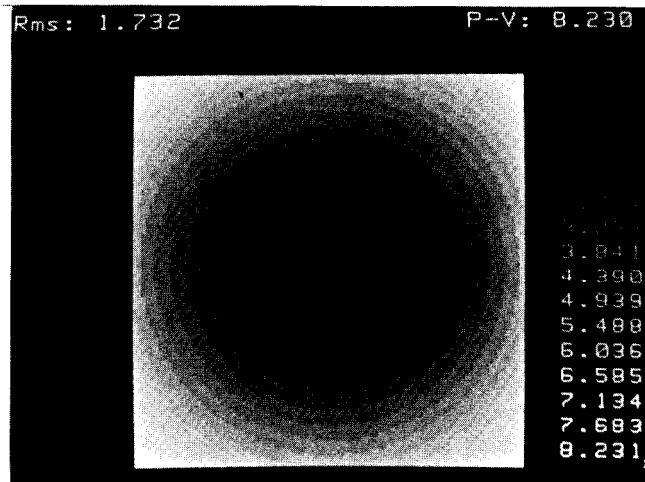


(a)

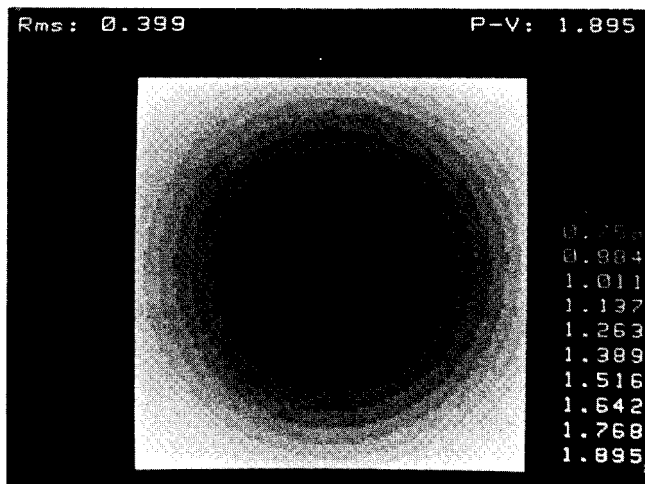


(b)

Figure 2. Phase maps for an aspheric surface having a few waves of aberration with tilt subtracted. (a) Single-wavelength result at  $0.6328 \mu\text{m}$ . (b) Two-wavelength result at equivalent wavelength  $2.13 \mu\text{m}$ .



(a)

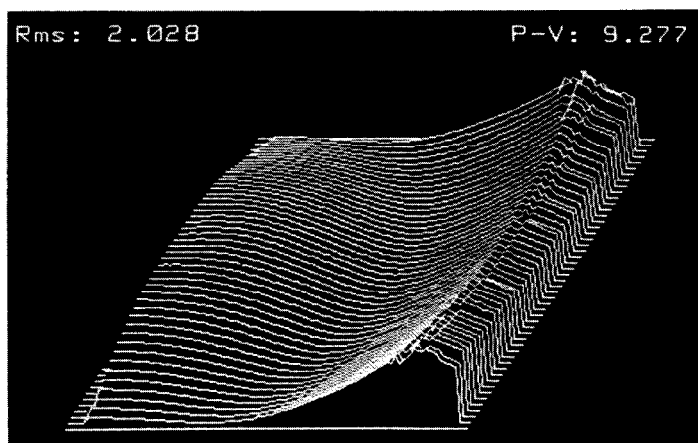


(b)

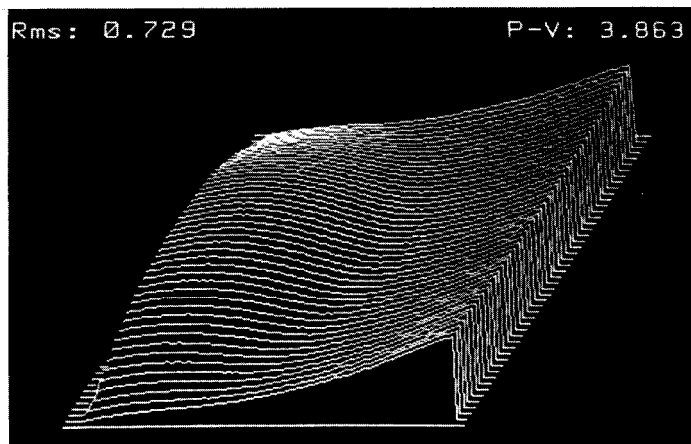
Figure 3. Phase maps for a spherical surface having a few waves defocus, and no imaging or null lenses present with tilt subtracted. (a) Single-wavelength result at  $0.6328 \mu\text{m}$ . (b) Two-wavelength result at equivalent wavelength  $2.75 \mu\text{m}$ .

between some adjacent pixels for the wavefront. When the two-wavelength technique is applied, the  $2\pi$  ambiguities are not a problem, and the phase map of the surface does not have discontinuities present in the single-wavelength case (figure 4 (b)). Another example is shown in figure 5. The phase map obtained using a single wavelength has discontinuities present over most of the wavefront. With two wavelengths, the phase map does not contain discontinuities.

The peak-to-valley repeatability of this technique is  $\lambda/15$  at the equivalent wavelength, with an r.m.s. repeatability of  $\lambda/100$ . The repeatability at the equivalent wavelength is the same as that measured for one wavelength, and TWPSI will contour steeper wavefronts than is possible with a single wavelength. Thus, this test will determine the contour of an aspheric surface to within an r.m.s. of  $\lambda_{eq}/100$ , which corresponds to a single wavelength test precision of  $\lambda_s/30$ .



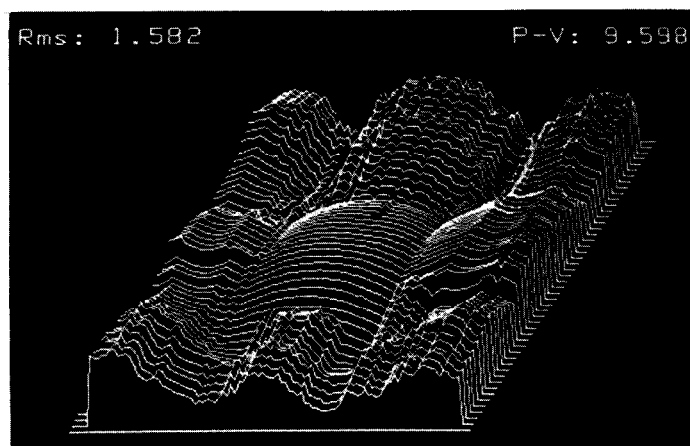
(a)



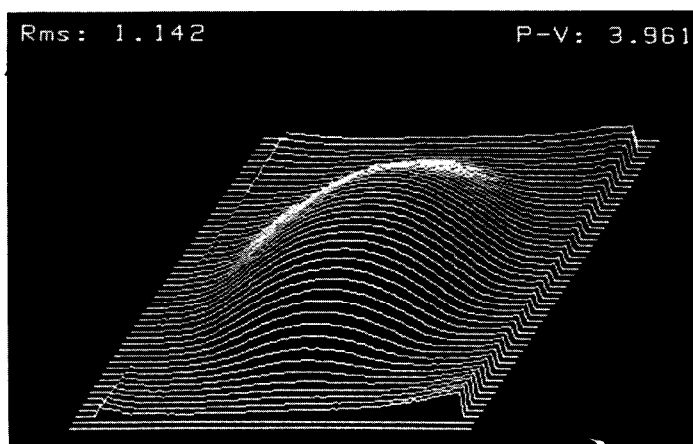
(b)

Figure 4. Three-dimensional contour maps for off-axis section of aspheric surface having many waves of aberration (tilt subtracted). (a) Single-wavelength phase at  $0.6328 \mu\text{m}$ . (b) Two-wavelength phase at equivalent wavelength  $2.75 \mu\text{m}$ .





(a)



(b)

Figure 5. Three-dimensional contour maps for on-axis section of aspheric surface having many waves of aberration (tilt subtracted). (a) Single-wavelength phase at  $0.6328 \mu\text{m}$ . (b) Two-wavelength phase at equivalent wavelength  $2.75 \mu\text{m}$ .

#### 4. Conclusions

Two-wavelength techniques are very valuable for the testing of steep surfaces such as aspheres because of the variable measurement sensitivity that is achieved by changing the wavelengths. The technique presented in this paper is straightforward and easy to implement. Its precision is limited by the equivalent wavelength. In order to increase the precision of the measurement, the single-wavelength phase data could have its  $2\pi$  ambiguities resolved using the integrated two-wavelength phases. The range of the measurement can be increased by using point detectors to sample fringes with a closer spacing than the detector size. Since the interferograms at each wavelength are recorded and then combined inside the computer, the intermediate recording step of two-wavelength holography is unnecessary: this makes the technique more convenient than TWH as a means of testing. The use of a computer

#### **1464 Contouring surfaces using two-wavelength phase-shifting interferometry**

means there are no errors due to fringe digitization, and further analysis on the phase data may easily be done. The technique of manipulating primary interferograms inside a computer to produce a secondary interferogram from double-exposure measurements has many applications besides TWPSI, one of which is phase measurement with double-exposure holography.

#### **References**

- [1] WYANT, J. C., 1971, *Appl. Opt.*, **10**, 2113.
- [2] KOLIOPOULOS, C. L., 1981, Ph.D. Dissertation, University of Arizona.
- [3] HAYES, J. B., 1984, Ph.D. Dissertation, University of Arizona.
- [4] CHENG, Y.-Y., and WYANT, J. C., 1984, *Appl. Opt.*, **23**, 4539.
- [5] CARRÉ, P., 1966, *Metrologia*, **2**, 13.